Bioluminescence imaging of mitochondrial Ca^{2+} dynamics in soma and neurites of individual adult mouse sympathetic neurons

Lucía Núñez, Laura Senovilla, Sara Sanz-Blasco, Pablo Chamero, María T. Alonso, Carlos Villalobos and Javier García-Sancho

Instituto de Biología y Genética Molecular (IBGM), Universidad de Valladolid and Consejo Superior de Investigaciones Científicas (CSIC), c/Sanz y Forés s/n, 47003 Valladolid, Spain

Changes in the cytosolic Ca^{2+} concentration ($[Ca^{2+}]_c$) are essential for triggering neurotransmitter release from presynaptic nerve terminals. Calcium-induced Ca^{2+} release (CICR) from the endoplasmic reticulum (ER) may amplify the $[Ca^{2+}]_c$ signals and facilitate neurotransmitter release in sympathetic neurons. In adrenal chromaffin cells, functional triads are formed by voltage-operated Ca^{2+} channels (VOCCs), CICR sites and mitochondria. In fact, mitochondria take up most of the Ca^{2+} load entering the cells and are essential for shaping $[Ca^{2+}]_c$ signals and exocytosis. Here we have investigated the existence of such functional triads in sympathetic neurons. The mitochondrial Ca^{2+} concentration ($[Ca^{2+}]_m$) in soma and neurites of individual mouse superior cervical ganglion (SCG) neurons was monitored by bioluminescence imaging of targeted aequorins. In soma, Ca^{2+} entry through VOCCs evoked rapid, near millimolar $[Ca^{2+}]_m$ increases in a subpopulation of mitochondria containing about 40% of the aequorin. Caffeine evoked a similar $[Ca^{2+}]_m$ increase in a mitochondrial pool containing about 30% of the aequorin and overlapping with the VOCC-sensitive pool. These observations suggest the existence of functional triads similar to the ones described in chromaffin cells. In neurites, mitochondria were able to buffer $[Ca^{2+}]_c$ increases resulting from activation of VOCCs but not those mediated by caffeine-induced Ca^{2+} release from the ER. The weaker Ca^{2+} buffering by mitochondria in neurites could contribute to facilitate Ca^{2+}-induced exocytosis at the presynaptic sites.

(Resubmitted 13 December 2006; accepted after revision 18 January 2007; first published online 18 January 2007)
Corresponding author L. Núñez : Instituto de Biología y Genética Molecular (IBGM), Universidad de Valladolid and CSIC, c/ Sanz y Forés s/n, 47003 Valladolid, Spain. Email: nunezl@ibgm.uva.es

Calcium signals govern important processes in neurons, including neurotransmitter release, membrane excitability, neurite outgrowth and neurodegeneration (Clapham, 1995; Ghosh & Greenberg, 1995). The cytosolic Ca^{2+} concentration ($[Ca^{2+}]_c$) increases upon activation of plasma membrane Ca^{2+} channels or Ca^{2+} release from intracellular stores (Berridge, 1998). In addition, Ca^{2+} signals can be amplified by release of Ca^{2+} from the endoplasmic reticulum (ER) through Ca^{2+}-induced Ca^{2+} released (CICR; Thayer *et al.* 1988; Hernández-Cruz *et al.* 1990; Friel & Tsien, 1992), mediated by ryanodine receptors (RyRs). Cytoplasmic organelles also participate in Ca^{2+} signalling (Alvarez *et al.* 1999). It is becoming increasingly clear that, besides its central role in cell energetics (Robb-Gaspers *et al.* 1998), mitochondria modulate cytosolic Ca^{2+} homeostasis (Herrington *et al.* 1996). Mitochondria can take up Ca^{2+} through the mitochondrial Ca^{2+} uniporter (Gunter & Pfeiffer, 1990; Kirichok *et al.* 2004), a high-capacity, low-affinity Ca^{2+} transport that activates exponentially with the increase of $[Ca^{2+}]$ in the surrounding cytosol (Gunter & Pfeiffer, 1990; Rizzuto *et al.* 1993; Montero *et al.* 2000). It has been reported that mitochondria can take up Ca^{2+} with relatively modest increases of $[Ca^{2+}]$ in the bulk cytosol (Herrington *et al.* 1996; Villalobos *et al.* 2002). In particular, mitochondria seem able to buffer physiological Ca^{2+} loads in neurons, and activation is paralleled by the increase of mitochondrial calcium concentration ($[Ca^{2+}]_m$; Werth & Thayer, 1994; Babcock *et al.* 1997). This probably results from the generation of subcellular high-Ca^{2+} domains at sites of Ca^{2+} entry or Ca^{2+} release (Rizzuto *et al.* 1993; Xu *et al.* 1997; Duchen, 1999; Montero *et al.* 2000), and mitochondrial uptake is much faster at these high-Ca^{2+} microdomains. Thus, Ca^{2+}

 DOI: 10.1113/jphysiol.2006.126524

uptake by mitochondria is favoured in mitochondria located strategically near Ca^{2+} hot spots, such as the mouth of Ca^{2+} channels or ryanodine and/or inositol 1,4,5-trisphosphate (IP_3) receptors. We have reported that, in chromaffin cells, a subpopulation of mitochondria is strategically and functionally coupled to both Ca^{2+} entry through voltage-operated Ca^{2+} channels (VOCCs) and Ca^{2+} release from intracellular stores, whereas the remaining mitochondria are located far away from these Ca^{2+} hot spots (Montero *et al.* 2000). The former mitochondrial subpopulation takes up larger Ca^{2+} loads, approaching millimolar levels, during cell stimulation (Montero *et al.* 2000; Villalobos *et al.* 2001). In fact, quantitative analysis of Ca^{2+} redistribution among different cytoplasmic compartments in chromaffin cells has demonstrated that most of the Ca^{2+} entering through VOCCs or released from ER by CICR is, in the short term, removed from the cytosol by mitochondria rather than by the other Ca^{2+} extruding systems (Villalobos *et al.* 2002). Consistently, prevention of mitochondrial Ca^{2+} uptake enhanced both the $[Ca^{2+}]_c$ rise and exocytosis (Montero *et al.* 2000). Therefore, strategically located mitochondria modulate the $[Ca^{2+}]_c$ signals and make possible the coexistence of high subplasmalemmal Ca^{2+} levels favouring exocytosis with a much lower $[Ca^{2+}]_c$ at the cell core. This is attained by avoiding spread of the entering Ca^{2+} load towards the cell core. In addition, intramitochondrial Ca^{2+} stimulates cellular respiration and tunes ATP synthesis to the increased requirements during the active state. The functional units or triads formed by VOCCs, RyRs and mitochondria seem essential for correct organization of the secretory process in adrenal chromaffin cells (Montero *et al.* 2000). Whether such functional units are present in neurons has not been investigated, perhaps owing to the difficulty of monitoring aequorin bioluminescence in single neurons. Here we combine the superb selectivity of targeted aequorin, the high expression induced by a viral vector (Alonso *et al.* 1998) and the high sensitivity provided by a photon-counting camera (Frawley *et al.* 1994; Rutter *et al.* 1996; Villalobos *et al.* 2002) to resolve changes of $[Ca^{2+}]_m$ at the single-cell level and even at the subcellular level (cell body and neurites).

Methods

Primary culture of sympathetic neurons from adult mouse superior cervical ganglion

The cell culture method was a modification of a previously described protocol (Martínez *et al.* 2002). Adult (8–12 weeks old) male Balb/c mice were fed *ad libitum* and maintained under a standard 12 h light–12 h dark photoregime. Experiments were conducted following the Guidelines of the Animal Care Committee and the Commission d'Ethique d'Experimentation Animale of the University of Lovain School of Medicine. Groups of four or five animals were killed by cervical dislocation and their superior cervical ganglia (SCG) rapidly removed under sterile conditions and transferred to a Petri dish containing ice-cold, Ca^{2+}- and Mg^{2+}-free Hank's balanced salt solution (HBSS). Ganglia were incubated for 10 min in HBSS containing collagenase (1.6 mg ml^{-1}) at 37°C, washed and incubated again in HBSS containing trypsin (1 mg ml^{-1}) for 15 min at 37°C. After gentle mechanical disruption with a siliconized, fire-polished Pasteur pipette, the cells were suspended in Dulbecco's modified Eagle's medium (DMEM) containing 10% fetal bovine serum (FBS), washed twice and suspended in culture medium (DMEM supplemented with 10% FBS and 50 ng ml^{-1} of nerve growth factor, NGF). Aliquots of the cell suspension (25 μl) were plated on poly L-lysine-coated 12 mm diameter glass coverslips. On average, we obtained the same number of cell-containing coverslips as ganglia dispersed. Cells were allowed to attach for 1 h and then an additional 300 μl of culture medium was added to each well and culture was continued for 2 days before the experiments.

Measurements of cytosolic $[Ca^{2+}]$ by fluorescence microscopy

The cells were loaded with fura-2 by incubation with fura-2 AM (4 μM) for about 1 h at room temperature in a standard medium of the following composition (mM): NaCl, 145; KCl, 5; $MgCl_2$, 1; $CaCl_2$, 1; glucose, 10; and sodium-Hepes, 10; pH 7.4 (adjusted with NaCH). Cells were then washed with the same medium, placed in a thermostatically controlled (37°C) chamber on the stage of an inverted microscope (Nikon Diaphot) and perfused with standard medium, prewarmed at 37°C. Cells were epi-illuminated alternately at 340 and 380 nm, and light emitted above 520 nm was recorded using a Magical Image processor (Applied Imaging, Newcastle, UK). Pixel-by-pixel ratios of consecutive frames were captured, and $[Ca^{2+}]_c$ values were estimated from these ratios by comparison with fura-2 standards. Other details were as reported previously (Núñez & García-Sancho, 1996; Villalobos *et al.* 2002).

Expression of aequorins

Mitochondria-targeted wild-type aequorin (mitAEQ) and low-Ca^{2+}-affinity, mutated aequorin (mitmutAEQ) were delivered using defective herpes simplex virus type 1 (HSV-1) amplicons prepared, packed and titrated as previously described (Alonso *et al.* 1998; Montero *et al.* 2000). The range of Ca^{2+} sensitivities for these aequorins has been published elsewhere (Montero *et al.* 2000). The native aequorin can discriminate different Ca^{2+}

concentrations within the 0.1–10 μM range, whereas the low-Ca^{2+}-affinity, mutated aequorin can distinguish different Ca^{2+} concentrations from the tens of micromolar to the low millimolar range when used in combination with celenterazine n. Cells were infected with 1×10^3 to 3×10^3 infectious virus particles per coverslip of the HSV-1 containing the corresponding aequorin gene and cultured for 18 h before measurements. Infection efficiency ranged between 50 and 85% (mean ± S.E.M., 67 ± 3%; 120 cells from 18 experiments). The correct targeting of aequorins to mitochondria has been reported elsewhere (Montero *et al.* 2000) and was confirmed here (results not shown).

Imaging of aequorin bioluminescence

Cells expressing the apoaequorins were incubated for 1–2 h at room temperature with 1 μM coelenterazine. Coelenterazine n was used in some experiments for reconstitution of the low-Ca^{2+}-affinity mutmitAEQ. Cells were placed into a perfusion chamber thermostatically regulated to 37°C under a Zeiss Axiovert 100 TV microscope and perfused at 5–10 ml min^{-1} with the test solutions, based on the standard perfusing solution described above, prewarmed at 37°C. At the end of each experiment, cells were permeabilized with 0.1 mM digitonin in 10 mM $CaCl_2$ to release all the residual aequorin counts. Bioluminescence images were taken with a Hamamatsu VIM photon counting camera handled with an Argus-20 image processor and integrated for 10 s periods. Photons per cell in each image were quantified using the Hamamatsu Aquacosmos software. Total counts per cell ranged between 2×10^3 and 2×10^5 and noise was (mean ± S.D.) 1 ± 1 counts s^{-1} per typical cell area (2000 pixels). Data were first quantified as rates of photoluminescence emission divided by the total counts remaining at each time and divided by the integration period (L/L_{total} in s^{-1}). Emission values of less than 4 counts s^{-1} were not used for calculations. Calibrations in terms of $[Ca^{2+}]_m$ were performed using the constant's values published previously (Alvarez & Montero, 2001). A bright field image was also taken at the beginning of each experiment. Further details have been reported previously (Villalobos *et al.* 2001, 2005).

Confocal microscopy

To identify endoplasmic reticulum and mitochondria in living sympathetic neurons, we first transiently expressed a fused green fluorescent protein (GFP) targeted to the ER. Endoplasmic reticulum–GFP contain in-frame fusion of enhanced green fluorescent protein (EGFP) and a Lys-Asp-Glu-Leu (KDEL) ER retention sequence in the herpes simplex virus plasmid (pHSV) amplicon vector. Expression was achieved by infecting cells with a defective HSV-1 containing the ER–GFP–aequorin gene and cultured for 18 h before measurements. Then, cells were loaded with Mitotracker Red® (200 nM) for 30 min at 37°C and washed with standard incubation medium. Confocal images were obtained using a Bio-Rad laser scanning system (Radiance 2100) coupled to a Nikon eclipse TE2100U inverted microscope with ×63 oil immersion objective (N.A. = 1.4). Green fluorescent protein was excited by the 488 nm laser line and emission was collected through a 500–560 nm bandpass filter. Mitotracker Red® was excited at 543 nm, and emitted light was collected through a 590 nm long-pass filter.

Results

In a first series of experiments, we studied the effects of both Ca^{2+} entry from the extracellular medium and Ca^{2+} release from the intracellular stores on $[Ca^{2+}]_m$. Calcium entry was induced by stimulation with high-K^+ solution, which depolarizes the plasma membrane and opens VOCCs. Calcium release from the ER was induced by stimulation of the ryanodine receptors with caffeine (Thayer *et al.* 1988; Hernández-Cruz *et al.* 1995). In all cases, we measured the changes of the $[Ca^{2+}]_c$ using fura-2 (Villalobos *et al.* 2002) and the changes of $[Ca^{2+}]_m$ with different aequorins (Montero *et al.* 2000). Both measurements were performed in the soma of the sympathetic neurons.

Figure 1 summarizes the effects of repetitive stimulation with high K^+. Use of fura-2 produced reproducible increases of $[Ca^{2+}]_c$, whose size varied between 800 and 2000 nM from cell to cell (Fig. 1*A*). In contrast, bioluminescence imaging of mitochondria-targeted aequorin (Montero *et al.* 2000; Villalobos *et al.* 2001) produced very different effects for the first stimulation and for subsequent ones (Fig. 1*B*). Since aequorin is burned out during the high-$[Ca^{2+}]$ periods (Shimomura *et al.* 1993; Alvarez & Montero, 2001; Villalobos *et al.* 2001), aequorin consumption provides a realistic record of what has happened each time, not biased by any calculation. The first stimulus consumed 44 ± 3% of the total photonic emissions (mean ± S.E.M. of 35 cells in 17 experiments). Aequorin consumption could be prevented by collapsing the mitochondrial membrane potential with the protonophore carbonyl cyanide p-(trifluoromethoxy) phenylhydrazone (FCCP) (data not shown), confirming that it results from mitochondrial Ca^{2+} uptake. The second and subsequent K^+ pulses released only 3 ± 1% of the total photons (Fig. 1*B*). The remaining photonic emissions could be released easily by permeabilizing the plasma membrane with digitonin and perfusing these permeabilized cells with solutions containing high levels of Ca^{2+} (> 20 μM; Fig. 1*B* and results not shown). The bottom part of Fig. 1*B* shows the calibrated $[Ca^{2+}]_m$ values. Apparently, the first stimulus produced a large $[Ca^{2+}]_m$ increase, whereas subsequent ones had a much smaller effect.

The outcome of these experiments is similar to previous findings in chromaffin cells (Montero *et al.* 2000; Villalobos *et al.* 2002), and we interpret them in terms of the existence of two mitochondrial pools with different spatial locations. The first pool, probably closer to the mouth of the Ca^{2+} channels at the plasma membrane, senses the high $[Ca^{2+}]$ concentrations built up in the high-Ca^{2+} microdomains. These mitochondria take up large amounts of Ca^{2+} that burns up all the aequorin very quickly during the first stimulus. During subsequent stimuli, this subplasmalemmal mitochondrial pool does not emit photoluminescence because all the aequorin contained therein was burned during the first stimulus. The second mitochondrial pool is closer to the cell core and would sense smaller $[Ca^{2+}]_c$ increases, of the same order of magnitude as the 'averaged' values found using fura-2. These mitochondria take up smaller amounts of Ca^{2+} and emit a much weaker photoluminescence signal, which is concealed during the first stimulus by the signal coming from the first mitocondrial pool. During the second and third stimuli, when all the aequorin from the first mitochondrial pool has burned out, the smaller

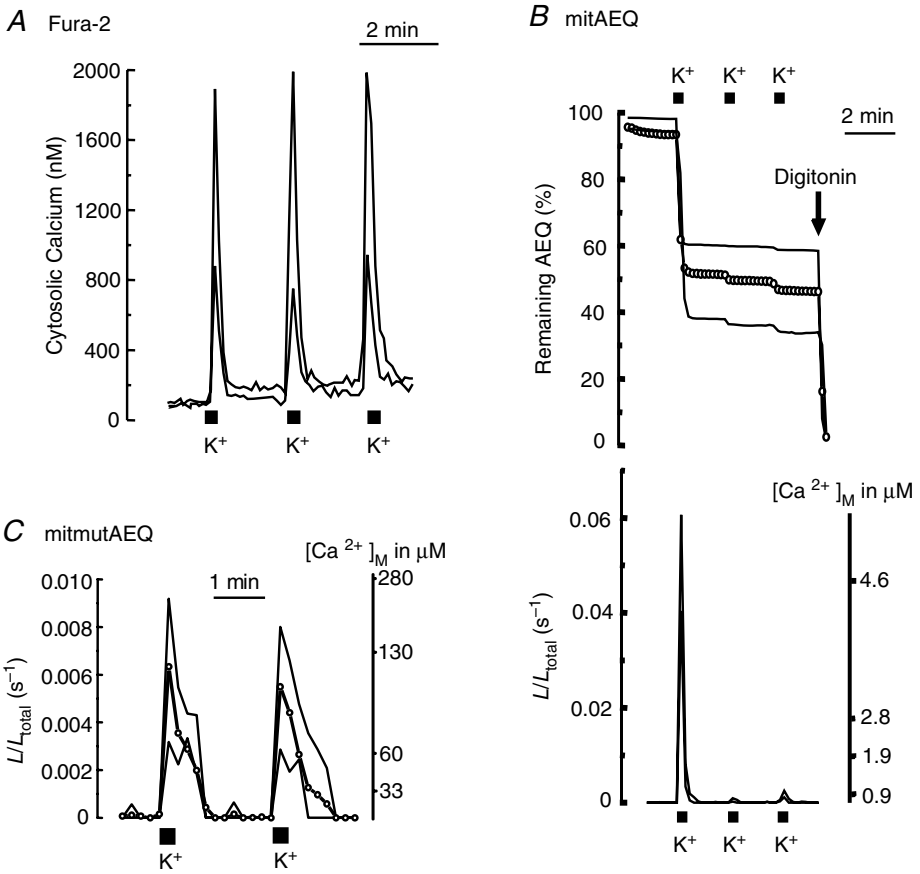

Figure 1. Effects of repeated stimulation of sympathetic neurons by depolarization with high K^+ on cytosolic and mitochondrial $[Ca^{2+}]$

Cells were repeatedly stimulated by perfusion with high K^+ solution (150 mM; 10 s pulses every 2 min). *A*, sympathetic neurons loaded with fura-2. $[Ca^{2+}]_c$ traces from two representative neurons (large and small response) are shown. Sixty-four consecutive fura-2 fluorescence images taken at either 340 or 380 nm excitation were captured, averaged and ratioed by hardware every 5 s. The image size was 256 × 256 pixels and the spatial resolution was 1 μm per pixel. Results are representative of 15 similar experiments. *B*, sympathetic neurons infected with mitAEQ and subjected to photon counting imaging. The upper traces show AEQ consumption in two representative neurons (large and small response), and open circles show the average value of 7 neurons present in the same microscopic field. The lower traces show calibrated signals (two single cells) from the same experiment. Data are representative of 17 similar experiments. *C*, sympathetic neurons were infected with mitmutAEQ and reconstituted with coelenterazine n (the low-Ca^{2+}-affinity system; see Methods). Data were corrected for the pool size (44% of the total AEQ counts). The traces corresponding to two extreme individual cells (large and small response) and the average of 5 cells present in the same microscope field (open circles) are shown. Only photonic emissions from the neuron cell body were counted for quantification of $[Ca^{2+}]_m$. Data are representative of 7 similar experiments.

signals coming from the core mitochondria show up (Fig. 1*B*).

In order to test the validity of this interpretation, we studied the effects of the same sequential stimuli in cells expressing mitmutAEQ reconstituted with coelenterazine n. This low-Ca^{2+}-affinity aequorin (Montero *et al.* 2000) would not be burned out completely during the first stimulus, and should then report the real and reproducible $[Ca^{2+}]_m$ responses to repetitive stimuli. Confirmation of this prediction is shown in Fig. 1*C*. This panel shows the calibrated $[Ca^{2+}]_m$ recordings of two representative individual cells (the ones with the strongest and the smallest response) and the average value of five cells present in the same microscopic field. Note that the responses were similar during the first and second stimuli, reaching $[Ca^{2+}]_m$ values that ranged between 100 and 300 μM. Note also that at such high Ca^{2+} concentrations the wild-type aequorin would be fully burned within a few seconds, since the half-consumption time is below 1 s at these saturating Ca^{2+} concentrations (Shimomura *et al.* 1993; Alvarez & Montero, 2001). The $[Ca^{2+}]_m$ peaks reached in the core mitochondrial pool, as shown by the wild-type aequorin during the second and the third high-K^+ stimuli, were much smaller (about 1 μM; Fig. 1*B*) and therefore should not be sensed by the low-Ca^{2+}-affinity mutmitAEQ.

Experiments to assess the gross properties of the mitochondrial Ca^{2+} uniporter in these neurons were performed in digitonin-permeabilized cells perfused with intracellular-like solutions containing different Ca^{2+} concentrations (Montero *et al.* 2000). Representative results are shown in Fig. 2. The low-Ca^{2+}-affinity aequorin (mitmutAEQ) almost failed to detect noticeable mitochondrial uptake at Ca^{2+} concentrations below 2 μM, but emitted quickly and uniformly more than 90% of the photonic emissions at 5 μM $[Ca^{2+}]$, and this was prevented by FCCP (not shown). Thus, although mitochondrial Ca^{2+} uptake at cytosolic Ca^{2+} concentrations below 2 μM might occur, it would not be detected with the low-Ca^{2+}-affinity aequorin with a sensitivity limit for $[Ca^{2+}]$ in the low micromolar range. As we have discussed elsewhere, the steepness of the Ca^{2+} dependence of the mitochondrial Ca^{2+} uniporter, together with the second-order dependence of the light emission on $[Ca^{2+}]$, stresses the abruptness of the transition from non-perceptible to massive mitochondrial uptake (Alonso *et al.* 2006). When high-Ca^{2+}-affinity aequorin is used, some Ca^{2+} uptake is measured also at 1 μM $[Ca^{2+}]_c$ and even below (Villalobos *et al.* 2002). In any case, these results indicate that the properties of the mitochondrial Ca^{2+} uniporter in sympathetic neurons are similar to those reported in other tissues (Gunter & Pfeiffer, 1990; Villalobos *et al.* 2002) and that high-Ca^{2+} microdomains stimulate mitochondrial uptake (Villalobos *et al.* 2002). Even more important, the fact that all the aequorin is consumed uniformly and homogeneously in the permeabilized cells indicates that the two mitochondrial pools, the subplasmalemmal and the core-located one, are both equally able to take up Ca^{2+} and that the differences seen in the intact cells do not result from their Ca^{2+} transport properties but from their spatial location.

Next, we studied the effects of repetitive stimulation with caffeine. Caffeine opens ER channels by activation of RyRs and promotes Ca^{2+} release to the cytosol. Repetitive stimulation with caffeine (1 stimulus every 4 min) produced sharp and reproducible $[Ca^{2+}]_c$ peaks ranging, from cell to cell, between 500 and 900 nM in size (Fig. 3*A*; measured with fura-2). Figure 3*B* illustrates the results obtained in neurons expressing the wild-type mitochondrial aequorin. The first stimulus released $32 \pm 4\%$ of total photonic emissions (mean ± S.E.M. of 25 cells from 12 experiments). In contrast, the second and subsequent caffeine stimuli released only $2 \pm 1\%$ of the total photons. These results are similar to those obtained with sequential stimulation using high K^+ (Fig. 1). Likewise, we interpret these results in terms of two mitochondrial pools with different spatial locations, the first one close and the second one away from the sites of Ca^{2+} release (i.e. RyRs at ER). This first mitochondrial pool would take up a larger amount of Ca^{2+}, thus burning up all its aequorin very quickly. To confirm this view, we carried out new measurements using the mutated,

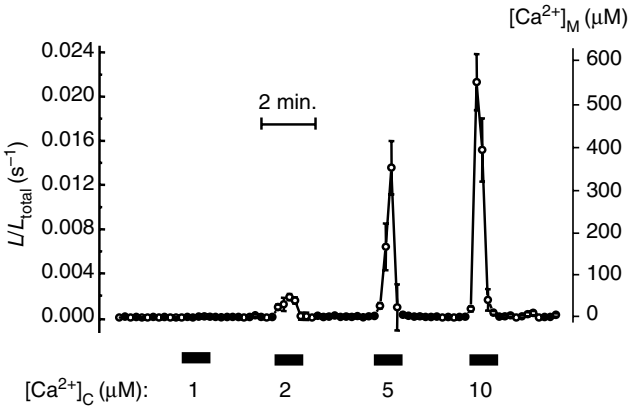

Figure 2. Ca^{2+} dependence of mitochondrial Ca^{2+} uptake in permeabilized sympathetic neurons
Sympathetic neurons infected with mitmutAEQ and reconstituted with coelenterazine n were permeabilized by treatment with 20 μM digitonin over 1 min at 37°C in Ca^{2+}-free (containing 0.2 mM EGTA) intracellular-like medium (composition, in mM: NaCl, 5; KCl, 130; $MgCl_2$, 2; KH_2PO_4, 2; Mg-ATP, 0.2; and potassium-Hepes, 20; pH 7.0 adjusted with KOH). Then the cells were perfused with 'intracellular-like' medium containing different $[Ca^{2+}]$ values, as shown in the figure. The different $[Ca^{2+}]$ values were obtained using buffers containing 1 mM EGTA or 1 mM N-(hydroxyethyl) ethylenediamine triacetic acid (HEDTA) and adjusting Ca^{2+} and Mg^{2+} as required (Patton *et al.* 2004). Values represent the mean ± S.E.M. of 5 different cells present in the same microscopic field. Results are representative of 5 similar experiments.

low-Ca^{2+}-affinity aequorin (mitmutAEQ reconstituted with coelenterazine n). Figure 3*C* shows that now each caffeine stimulus produced a similar output that, once corrected for the pool size (32%), revealed an increase of $[Ca^{2+}]_m$ of about 150 μM, a value close to the one achieved in the mitochondria sensing the VOCCs upon high-K^+ stimulation. These results suggest that Ca^{2+} release from ER by activation of ryanodine receptors generates subcellular high-$[Ca^{2+}]$ microdomains that are sensed only by a subpopulation of mitochondria, while the remainder sense much smaller Ca^{2+} concentrations.

We then asked whether the pool of mitochondria that sense Ca^{2+} entry and the one sensing Ca^{2+} release is the same or a different pool. To this end, neurons expressing the high-Ca^{2+}-affinity mitochondrial aequorin were subjected to photon counting imaging for $[Ca^{2+}]_m$ measurements after sequential stimulation, first with high K^+ and then with caffeine (Fig. 4*A*) or the same stimuli in the reverse order (Fig. 4*B*). After stimulation with high K^+ the effects of caffeine on mitAEQ consumption were very small, only 6 ± 1% of all the photons (mean ± S.E.M. of 17 cells from 7 experiments; Fig. 4*A*). When the protocol was performed in the reverse order, first stimulation with caffeine and then with high K^+, the consumption during the first K^+ stimulus was only 15 ± 2% of the total counts (21 cells in 12 experiments; Fig. 4*B*). This value is larger than with caffeine, but still much smaller than the one of about 40% obtained during the first stimulation with high K^+ when there was not previous stimulation with caffeine (Figs 1*B* and 4*A*). These results indicate that the subpopulation of mitochondria sensing the plasma membrane Ca^{2+} entry and the ER Ca^{2+} release have a large degree of overlap.

All the above observations refer to the mitochondria located in the soma. We then asked whether mitochondria located in the neurites would behave in a similar manner. To this end, we collected photonic emissions simultaneously in both neurites and soma of sympathetic neurons subjected to stimulation with high K^+ and/or caffeine. Figure 5*A* summarizes the effects on $[Ca^{2+}]_c$, measured with fura-2. The $[Ca^{2+}]_c$ increase induced by high K^+ was similar in soma and neurites (Fig. 5*A*, K^+ panel, and results not shown). Interestingly, the size of the $[Ca^{2+}]_c$ increases induced by caffeine was significantly

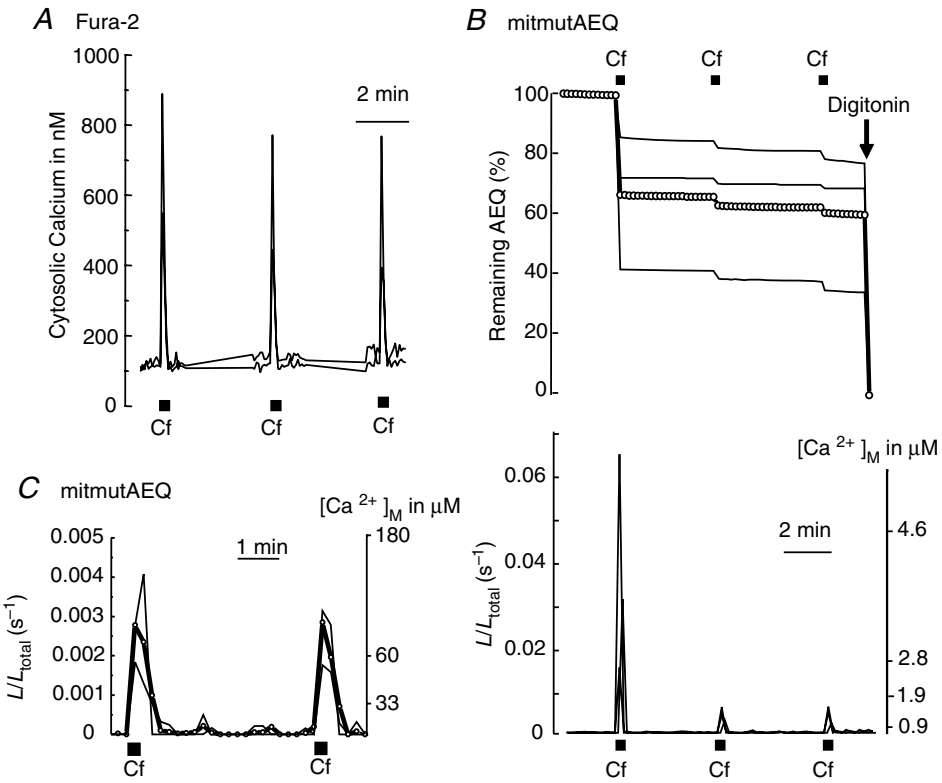

Figure 3. Effects of repeated stimulation with caffeine on $[Ca^{2+}]_c$ and $[Ca^{2+}]_m$
Sympathetic neurons were repeatedly stimulated with caffeine (Cf; 50 mM for 10 s every 4 min). *A*, effects on $[Ca^{2+}]_c$ measured with fura-2. Data are representative of 16 similar experiments. *B*, effects on $[Ca^{2+}]_m$ measured with mitAEQ (high-Ca^{2+}-affinity system). Data are representative of 12 similar experiments. *C*, effect on $[Ca^{2+}]_m$ measured with mutmitAEQ and coelenterazine n (low-Ca^{2+}-affinity system). Data are representative of 6 similar experiments. Other details as in Fig. 1.

larger in the neurites than in the soma (Fig. 5*A*, Caff panel and recordings). In four independent experiments, the mean $\Delta[Ca^{2+}]_c$ values obtained after stimulation with caffeine were (mean ± S.E.M. of 6 cells) 325 ± 8 nM in the soma and 435 ± 27 nM in the neurites, respectively. The differences were statistically significant ($P < 0.05$; Student's paired *t* test). However, the duration of the peak and the rates of $[Ca^{2+}]_c$ increase and decline were similar in the neurites and the soma.

In another set of experiments, the effects of sequential and repetitive stimulation with high K^+ and caffeine on $[Ca^{2+}]_m$ were measured using the mitochondrial aequorin (Fig. 5*B*). The outcome with high K^+ was not surprising. As already shown for the soma in another experiment (Fig. 3*B*), the second and third stimuli were scarcely effective, and previous stimulation with K^+ 'occluded' the further effect of caffeine. The behaviour in the neurites in response to stimulation with high K^+ was similar (Fig. 5*B*). The results with caffeine were, however, most unexpected, since the effect of caffeine on $[Ca^{2+}]_m$ was much smaller in the neurites than in the soma (Fig. 5*B*). Taken together, these results indicate that mitochondria in neurites are scarcely able to take up and buffer the Ca^{2+} released from the ER, even though they efficiently buffer the Ca^{2+} entering though VOCCs.

Finally, we attempted to quantify the relative contents of mitochondria and ER in both soma and neurites. To this end, sympathetic neurons were infected with a defective HSV-1 virus containing ER-targeted GFP. After 18 h of culture, these cells were loaded with Mitotracker Red® to selectively stain mitochondria and analysed by double-channel laser scanning confocal fluorescence microscopy (Fig. 5*C*). The amount of mitochondria relative to ER in both soma and neurites was quantified by dividing the Mitotracker Red® fluorescence signal coming from mitochondria by the green GFP fluorescence coming from the ER. The first two images in Fig. 5*C* show the labelling of mitochondria and ER, respectively, in two serial 1 μm optical sections (data representative of 18 cells). Mitochondria and ER were present in both the soma and the neurites. These results are in agreement with the ability to release aequorin photonic emissions from mitochondria-targeted aequorin both in the soma and in the neurites. The presence of ER at both locations, soma and neurites, is consistent with the ability of caffeine to increase $[Ca^{2+}]_c$ at both locations (Fig. 5*A*). The relative abundance of mitochondria and ER in soma and neurites was, however, not uniform. Mitochondria seemed to be more abundant in neurites, as shown by the more extensive red labelling at this location (see merged image in Fig. 5*C*). The average of red/green fluorescence ratio in soma and neurites in 10 independent experiments is summarized in the bar graph in Fig. 5*C*. The values have been normalized for each neuron with regard to the value in the soma. On

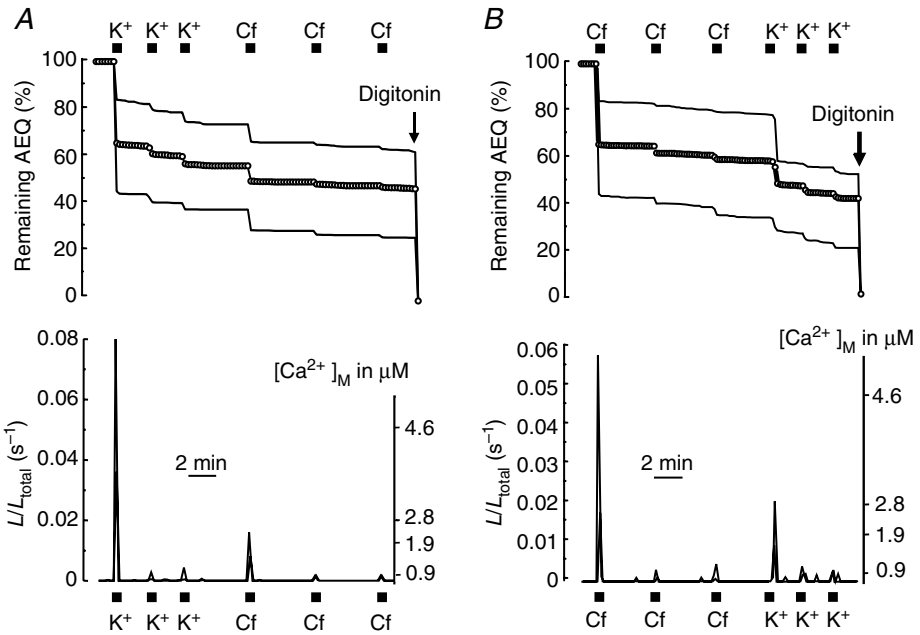

Figure 4. Overlap between the mitochondrial pools sensing Ca^{2+} entry through the plasma membrane and Ca^{2+} release from ER

Sympathetic neurons expressing the high-Ca^{2+}-affinity mitAEQ were repeatedly stimulated first with high K^+ and then with caffeine (Cf; *A*) or first with caffeine and then with high K^+ (*B*), as shown. The upper traces show aequorin consumption and lower traces show the calibrated signal. Values obtained in two extreme cells (large and small responses) and the average of all the cells present in the same microscope fields (circles) are shown. Data are representative of 7 (*A*) and 12 independent experiments (*B*).

average, the mitochondria/ER ratio in the neurites was almost twice as large as in the soma ($P < 0.001$).

Discussion

Single-cell photon counting imaging of targeted aequorins reveals that mitochondria take up large amounts of Ca^{2+} during stimulation of mouse sympathetic neurons. Since mitochondrial aequorin is consumed when $[Ca^{2+}]_m$ increases, the history of the different mitochondrial pools that contribute to Ca^{2+} accumulation during repetitive stimulation could be traced (Montero *et al.* 2000; Villalobos *et al.* 2002). As in chromaffin cells (Montero

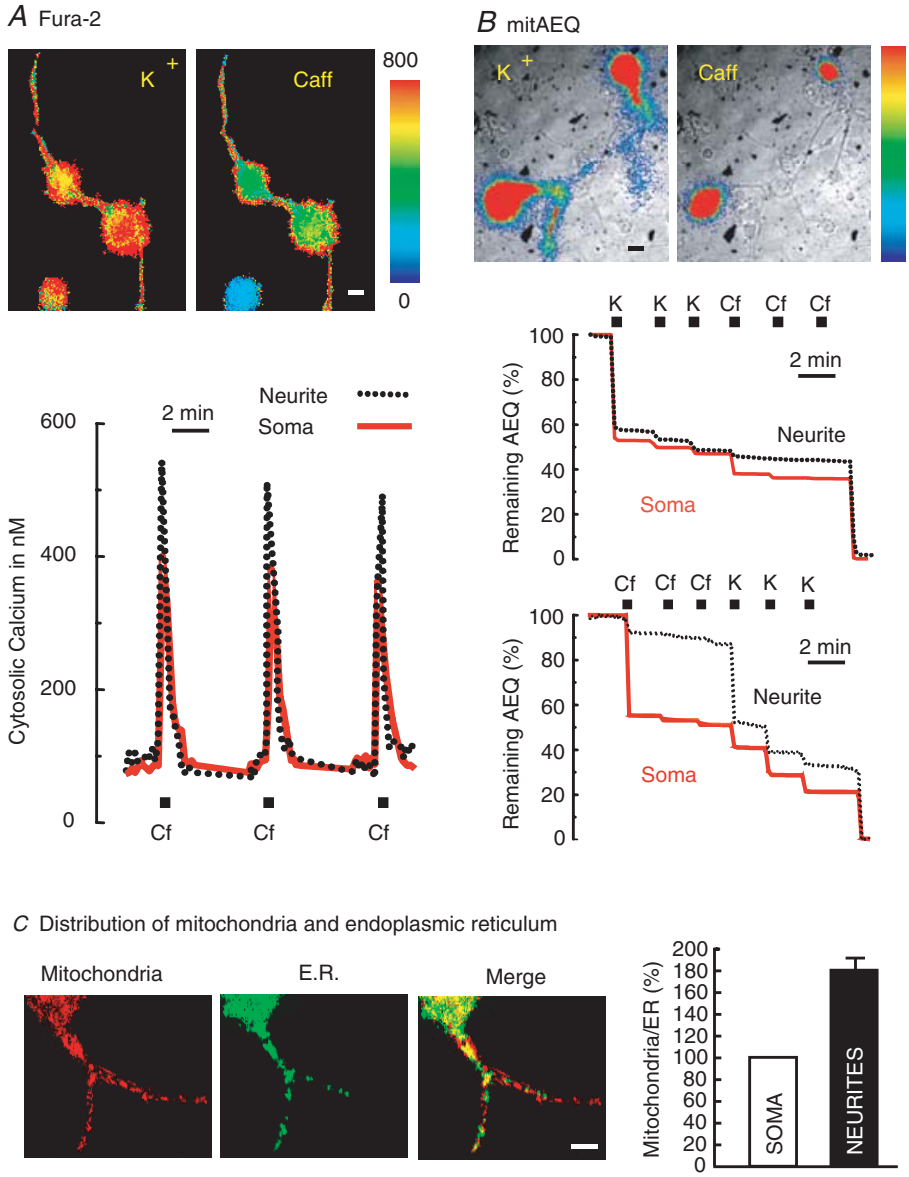

Figure 5. Differential effects of stimulation with high K^+ and caffeine in the cell body and the neurites
A, effects on $[Ca^{2+}]_c$ measured with fura-2 as described in Methods. Sixty-four 256 × 256 pixel images at alternate excitation wavelengths (340 and 380 nm) were averaged and ratioed by hardware every 5 s. Spatial resolution was of 1 μm per pixel. Results are representative of 4 similar experiments. *B*, effects on $[Ca^{2+}]_m$ measured with mitAEQ (high-Ca^{2+}-affinity system). The first high-K^+ stimulation released 37 ± 4% of the total photonic emissions in neurites; the second and subsequent stimuli released 3 ± 1% (mean ± S.E.M. of 20 cells from 15 experiments). The first caffeine stimulus induced a very small aequorin consumption in neurites (5 ± 1% of total photonic emissions; mean ± S.E.M. of 22 cells from 16 experiments); the subsequent stimulation with high K^+ consumed 21 ± 2% of aequorin. Regions of interest for measurements were defined selectively either in soma or neurites. Other details are as in Figs 1 and 2. *C*, analysis of relative content of mitochondria and ER in soma and neurites of sympathetic neurons. A sample of confocal slicing of a neuron expressing ER-GFP (green) and loaded with Mitotracker Red® (red) and the merged image are shown. The right-hand panel compares the contents of soma and neurites for 12 neurons (mean ± S.E.M.). The values are expressed as mitochondria/ER ratio and were normalized to 100% for the soma content in each case (*$P < 0.001$). Bars in images represent 10 μM.

et al. 2000), most of the Ca^{2+} uptake takes place in a subpopulation of mitochondria, probably the ones closest to the sites of Ca^{2+} entry or Ca^{2+} release. The applicable dimensions have been estimated between 0.2 and 2 μm in adrenal chromaffin cells (Villalobos *et al.* 2002). These mitochondria would sense Ca^{2+} microdomains in which high enough concentrations are achieved to activate the low-affinity mitochondrial Ca^{2+} uniporter for fast transport inside the mitochondrial matrix. The progression of the Ca^{2+} wave towards the cell core is effectively shielded by this mitochondrial pool in such a way that the other mitochondrial pool senses and takes up much smaller amounts of Ca^{2+} (Figs 1 and 3). These results agree with previous studies using X-ray microanalysis, in which stimulated and rapidly frozen frog sympathetic neurons contained two different subpopulations of mitochondria with different Ca^{2+} levels (Pivovarova *et al.* 1999). This black and white view is somewhat artificial. A continuum of mitochondria with different Ca^{2+} uptakes must exist, but the transition between both ends of the population must be extremely steep because the rate of mitochondrial Ca^{2+} uptake depends exponentially on $[Ca^{2+}]_c$ (Gunter & Pfeiffer, 1990; Rizzuto *et al.* 1993; Montero *et al.* 2000). This real bimodality is further exaggerated by aequorin, whose luminescence emission also depends exponentially on $[Ca^{2+}]$ (Alonso *et al.* 2006). Thus, the low-affinity aequorin system senses almost exclusively the high-Ca^{2+} mitochondrial pool, whereas the high-affinity aequorin system is quickly burned in this pool and, after a while, only detects the low-Ca^{2+} mitochondrial pool. In this way, by buffering the Ca^{2+} load, mitochondria can shape the cytosolic Ca^{2+} signal and exocytosis (Herrington *et al.* 1996; Montero *et al.* 2000; Friel, 2000; Villalobos *et al.* 2002; David & Barrett, 2003). Previous observations showing that mitochondrial depolarization, a manoeuvre that limits mitochondrial Ca^{2+} uptake, results in increased $[Ca^{2+}]_c$ spikes induced by electric stimulation in sympathetic neurons (Peng, 1998; Friel, 2000) are consistent with this view. The mitochondrial pool sensing Ca^{2+} entry through VOCCs overlapped with the one that accumulated Ca^{2+} after Ca^{2+} release through RyRs. These results suggest that, as in chromaffin cells (Montero *et al.* 2000), plasma membrane channels, ER release sites and mitochondria group spatially in triads or functional units that activate jointly, regardless of whether the Ca^{2+} originates extra- or intracellularly. Consistent with this view, local Ca^{2+} release events evoked by low caffeine concentrations have recently been reported to take place near the plasma membrane in the soma of superior cervical ganglion neurons (Yao *et al.* 2006).

It has been proposed that, in addition to Ca^{2+} fluxes through Ca^{2+} channels at the plasma membrane or the ER, other modulatory processes may contribute to generate Ca^{2+} signals with specific spatial location (Johenning *et al.* 2002). In dorsal root ganglion (DRG) neurons, mitochondria seem to buffer Ca^{2+} entering through plasmalemmal channels more efficiently than Ca^{2+} released from the ER (Svichar *et al.* 1997). We have investigated here whether redistribution of Ca^{2+} among different subcellular compartments is similar in the soma and neurites inside single sympathetic neurons. Our bioluminescence imaging approach enables photonic emissions from mitochondria in soma and neurites to be dissected. As in the soma, the behaviour in neurites was not homogeneous with regard to VOCCs, and we identified two different populations of mitochondria. One pool accumulated large amounts of Ca^{2+}, whereas the other took up much smaller amounts. In contrast, the mitochondria in neurites differed from those in the soma in that they were not able to sense Ca^{2+} release induced by caffeine, as revealed by the high-Ca^{2+}-affinity aequorin (Fig. 5*B*). This did not result from a lack of RyRs in neurites, since caffeine was able to increase $[Ca^{2+}]_c$ at this location (Fig. 5*A*), and previous reports have also demonstrated the presence of functional RyRs in the presynaptic terminals of sympathetic neurons (Peng, 1996). In contrast, ER-directed GFP was also expressed in neurites (Fig. 5*C*). Thus, even though mitochondria are more abundant in neurites than in the soma (Fig. 5*C*), mitochondria in neurites are more loosely coupled to ER and do not efficiently buffer the Ca^{2+} released through RyRs. This may explain why the $[Ca^{2+}]_c$ signal induced by caffeine is larger in the neurites than in the soma (Fig. 5*A*). Interestingly, other authors have also reported that Ca^{2+} signals may be larger in neurites than in the soma in a variety of cell models (Svichar *et al.* 1997; Koizumi *et al.* 1999; Johenning *et al.* 2002; Yao *et al.* 2006). For example, interference of mitochondrial Ca^{2+} uptake with carbonyl cyanide m-chlorophenylhyrazone (CCCP) modulated $[Ca^{2+}]_c$ transients induced by Ca^{2+} entry through VOCC channels, but not those resulting from caffeine-induced release of Ca^{2+} from ER in DRG neurons (Svichar *et al.* 1997). In addition, the somatic Ca^{2+} response to carbachol in differentiated PC12 cells displayed a much shallower slope and smaller amplitude than the response obtained in the neurites (Johenning *et al.* 2002). These differences were not attributable to differences in the Ca^{2+} contents of the ER in the neurites and soma, and the authors suggested that additional, unrecognized modulatory processes are necessary to generate spatially specific calcium signals. Global Ca^{2+} signals in neurons are made of elementary signals, which have been studied in great detail in both differentiated PC12 cells (Koizumi *et al.* 1999) and superior cervical ganglion neurons (Yao *et al.* 2006). In fact, the so-called elementary events (Ca^{2+} sparks and glows) were reported to be larger and more frequent in the neurites than in the soma of these neurons (Yao *et al.* 2006). The larger responses of these neurites could be at least partly explained by the smaller Ca^{2+}-buffering

capacity of the mitochondria in the neurites. Our data are consistent with previous suggestions (Svichar *et al.* 1997) attributing the smaller buffering capacity to peculiar localization of mitochondria, far away from the ER release sites, rather than to functional differences in Ca^{2+} handling by the mitochondrial uniporter. Calcium-induced Ca^{2+} release is believed to play an important role in the action potential-evoked release of neurotransmitter in postganglionic sympathetic nerve terminals (Smith & Cunnane, 1996) and presynaptic neuromuscular terminals (Narita *et al.* 2000). We can speculate that the lack of mitochondria close enough to ER could result in local higher $[Ca^{2+}]_c$ increases at the synaptic sites. Thus, strategic location of mitochondria may shape cytosolic Ca^{2+} signals differentially in soma and neurites.

References

Alonso MT, Barrero MJ, Carnicero E, Montero M, García-Sancho J & Alvarez J (1998). Functional measurements of $[Ca^{2+}]$ in the endoplasmic reticulum using a herpes virus to deliver targeted aequorin. *Cell Calcium* **24**, 87–96.

Alonso MT, Villalobos C, Chamero P, Alvarez J & García-Sancho J (2006). Calcium microdomains in mitochondria and nucleus. *Cell Calcium* **40**, 513–525.

Alvarez J & Montero M (2001). Ca^{2+} measurements with luminescent proteins in the endoplasmic reticulum. In *Measuring Calcium and Calmodulin Inside and Outside Cells*, Springer Laboratory Manual,, ed. Petersen OH, pp. 147–163. Springer Verlag Berlin.

Alvarez J, Montero M & García-Sancho J (1999). Subcellular Ca^{2+} dynamics. *News Physiol Sci* **14**, 161–168.

Babcock DF, Herrington J, Park YB & Hille B (1997). Mitochondrial participation in the intracellular Ca^{2+} network. *J Cell Biol* **136**, 833–843.

Berridge MJ (1998). Neuronal calcium signaling. *Neuron* **21**, 13–26.

Clapham DE (1995). Calcium signaling. *Cell* **80**, 259–268.

David G & Barrett EF (2003). Mitochondrial Ca^{2+} uptake prevents desynchronization of quantal release and minimizes depletion during repetitive stimulation of mouse motor nerve terminals. *J Physiol* **548**, 425–438.

Duchen MR (1999). Contributions of mitochondria to animal physiology: from homeostatic sensor to calcium signaling and cell death. *J Physiol* **516**, 1–17.

Frawley LS, Faught WJ, Nicholson J & Moomaw B (1994). Real time measurement of gene expression in living endocrine cells. *Endocrinology* **135**, 468–471.

Friel DD (2000). Mitochondria as regulators of stimulus-evoked calcium signals in neurons. *Cell Calcium* **28**, 307–316.

Friel DD & Tsien RW (1992). A caffeine- and ryanodine-sensitive Ca^{2+} store in bullfrog sympathetic neurons modulates effects of Ca^{2+} entry on $[Ca^{2+}]$. *J Physiol* **450**, 217–246.

Ghosh A & Greenberg ME (1995). Calcium signaling in neurons: molecular mechanisms and cellular consequences. *Science* **268**, 239–247.

Gunter TE & Pfeiffer DR (1990). Mechanisms by which mitochondria transport calcium. *Am J Physiol Cell Physiol* **258**, C755–C786.

Hernández-Cruz A, Díaz-Muñoz M, Gómez-Chavarin M, Canedo-Merino R, Protti DA, Escobar AL, Sierralta J & Súarez-Isla BA (1995). Properties of the ryanodine-sensitive release channels that underlie caffeine-induced Ca^{2+} mobilization from intracellular stores in mammalian sympathetic neurons. *Eur J Neurosci* **7**, 1684–1699.

Hernández-Cruz A, Sala F & Adams PR (1990). Subcellular Ca^{2+} transients visualizad by confocal microscopy in a voltage-clamped vertebrate neuron. *Science* **247**, 858–862.

Herrington J, Park YB, Babcock DF & Hille B (1996). Dominant role of mitochondria in clearance of large Ca^{2+} loads from rat adrenal chromaffin cells. *Neuron* **16**, 219–228.

Johenning FW, Zochowski M, Conway SJ, Holmes AB, Koulen P & Ehrlich BE (2002). Distinct intracellular calcium transients in neurites and somata integrate neuronal signals. *J Neurosci* **22**, 5344–5353.

Kirichok Y, Krapivinsky G & Clapham DE (2004). The mitochondrial calcium uniporter is a highly selective ion channel. *Nature* **427**, 360–364.

Koizumi S, Bootman MD, Bobanovic LK, Schell MJ, Berridge MJ & Lipp P (1999). Characterization of elementary Ca^{2+} release signals in NGF-differentiated PC12 cells and hippocampal neurons. *Neuron* **22**, 125–137.

Martínez JA, Lamas JA & Gallego R (2002). Calcium current components in intact and dissociated adult mouse sympathetic neurons. *Brain Res* **951**, 227–236.

Montero M, Alonso MT, Carnicero E, Cuchillo-Ibáñez I, Albillos A, García AA, García-Sancho J & Alvarez J (2000). Chromaffin-cell stimulation triggers fast millimolar mitochondrial Ca^{2+} transients that modulate secretion. *Nature Cell Biol* **2**, 57–61.

Narita K, Akita T, Hachisuka J, Huang S, Ochi K & Kuba K (2000). Functional coupling of Ca^{2+} channels to ryanodine receptors at presynaptic terminals. Amplification of exocytosis and plasticity. *J Gen Physiol* **115**, 519–532.

Núñez L & García-Sancho J (1996). Two different constituents of plasma increase cytosolic calcium selectively in neurons or glia of primary rat cerebellar cultures. *J Physiol* **490**, 577–583.

Patton C, Thompson S & Epel D (2004). Some precautions in using chelators to buffer metals in biological solutions. *Cell Calcium* **35**, 427–431.

Peng Y (1996). Ryanodine-sensitive component of calcium transients evoked by nerve firing at presynaptic nerve terminals. *J Neurosci* **16**, 6703–6712.

Peng YY (1998). Effects of mitochondrion on calcium transients at intact presynaptic terminals depend on frequency of nerve firing. *J Neurophysiol* **80**, 186–195.

Pivovarova NB, Hongpaisan J, Andrews SB & Friel DD (1999). Depolarization-induced mitochondrial Ca^{2+} accumulation in sympathetic neurons: spatial and temporal characteristics. *J Neurosci* **19**, 6372–6384.

Rizzuto R, Brini M, Murgia M & Pozzan T (1993). Microdomains with high Ca^{2+} close to IP_3-sensitive channels that are sensed by neighboring mitochondria. *Science* **262**, 744–747.

Robb-Gaspers LD, Burnett P, Rutter GA, Denton RM, Rizzuto R & Thomas AP (1998). Integrating cytosolic calcium signals into mitochondrial metabolic responses. *EMBO J* **17**, 4987–5000.

Rutter GA, Burnett P, Rizzuto R, Brini M, Murgia M, Pozzan T, Tavaré JM & Denton RM (1996). Subcellular imaging of intramitochondrial Ca^{2+} with recombinant targeted aequorin: significance for the regulation of pyruvate dehydrogenase activity. *Proc Natl Acad Sci U S A* **93**, 5489–5494.

Shimomura O, Musicki B, Kishi Y & Inouye S (1993). Light-emitting properties of recombinant semi-synthetic aequorins and recombinant fluorescein-conjugated aequorin for measuring cellular calcium. *Cell Calcium* **14**, 373–378.

Smith AB & Cunnane TC (1996). Ryanodine-sensitive calcium stores involved in neurotransmitter release from sympathetic nerve terminals of the guinea-pig. *J Physiol* **497**, 657–664.

Svichar N, Kostyuk P & Verkhratsky A (1997). Mitochondria buffer Ca^{2+} entry but not intracellular Ca^{2+} release in mouse DRG neurons. *Neuroreport* **8**, 3929–3932.

Thayer SA, Hirning LD & Miller RJ (1988). The role of caffeine-sensitive calcium stores in the regulation of the intracellular free calcium concentration in rat sympathetic neurons in vitro. *Mol Pharmacol* **34**, 664–673.

Villalobos C, Nadal A, Núñez L, Quesada I, Chamero P, Alonso MT & García-Sancho J (2005). Bioluminescence imaging of nuclear calcium oscillations in intact pancreatic islets of Langerhans from the mouse. *Cell Calcium* **38**, 131–139.

Villalobos C, Núñez L, Chamero P, Alonso MT & García-Sancho J (2001). Mitochondrial $[Ca^{2+}]$ oscillations driven by local high $[Ca^{2+}]$ domains generated by spontaneous electric activity. *J Biol Chem* **276**, 40293–40297.

Villalobos C, Núñez L, Montero M, García AG, Alonso MT, Chamero P, Alvarez J & García-Sancho J (2002). Redistribution of Ca^{2+} among cytosol and organella during stimulation of bovine chromaffin cells. *FASEB J* **16**, 343–353.

Werth JL & Thayer SA (1994). Mitochondria buffer physiological calcium loads in cultured rat dorsal root ganglion neurons. *J Neurosci* **14**, 346–356.

Xu T, Naraghi M, Kang H & Neher E (1997). Kinetic studies of Ca^{2+} binding and Ca^{2+} clearance in the cytosol of adrenal chromaffin cells. *Biophys J* **73**, 532–545.

Yao L, Wang G, Ou-Yang K, Wei C, Wang X, Wang S, Yao W, Huang H, Luo J, Wu C, Liu J, Zhuan Z & Cheng H (2006). Ca^{2+} sparks and Ca^{2+} glows in superior cervical ganglion neurons. *Acta Pharmacol Sin* **7**, 848–852.

Acknowledgements

This work was supported by grants from Junta de Castilla y León (VA071/02; VA022A05), Ministerio de Educación y Ciencia (MEC; BFU2004-02764), Fondo de Investigaciones Sanitarias FIS 04/1510 and Ministerio de Sanidad, Instituto de Salud Carlos III, Red de Terapia Celular. L.N. is fellow of the Ramón y Cajal Program (MEC and FEDER-FSE). L.S. is the recipient of a predoctoral fellowship from MEC. Pablo Chamero held a predoctoral fellowship from the Basque Government.